International Journal of Scientific Research in Engineering and Management (IJSREM)
Volume: 10 Issue: 11 | Nov - 2026 SJIF Rating: 8.659 ISSN: 2582-3930

Spatiotemporal Assessment of Carbon Stock in the Melghat Forest Using Remote Sensing and GIS

Prof. S. V. Pawar[1]

Karunika Virghat[2], Sugat Sonule[3], Uday Kanthak[4], Vansh Ambekar[5], Vanshika Raghuvanshi[6].

[1]Assistant Professor, Department of Civil Engineering, P. R. Pote Patil College of Engineering & Management, Amravati, India

[2,3,4,5,6]Students, Department of Civil Engineering, P. R. Pote Patil College of Engineering & Management, Amravati, India

---

Abstract

Tropical dry deciduous forest ecosystems serve as vital terrestrial carbon sinks and regional watershed regulators, yet they exhibit extreme seasonal phenological fluctuations and vulnerability to peripheral anthropogenic fragmentation. Conventional ground-based forest inventories are labor-intensive and spatially sparse across rugged mountainous terrain. This paper presents an integrated geospatial methodology combining cloud-based remote sensing (Google Earth Engine) and Geographic Information System (QGIS) analytics with the Intergovernmental Panel on Climate Change (IPCC) Tier-2 area-based accounting framework to evaluate spatiotemporal carbon stock dynamics in the Melghat Forest (Melghat Tiger Reserve, 218,112.00 ha; 2,181.12 km^2), Amravati District, Maharashtra, India, from 2021 to 2025. Multi-temporal Sentinel-2 Multi-Spectral Instrument (MSI) Level-2A surface reflectance imagery (10 m spatial resolution) was acquired within a strict post-monsoon observation window (October 15–November 25; cloud cover <20%) to eliminate dry-season deciduous leaf fall bias. Normalized Difference Vegetation Index (NDVI) zonal statistics revealed a non-linear trajectory: mean NDVI rose from 0.314 (2021) to 0.585 (2022) and 0.644 (2023), dropped sharply to 0.286 in 2024 due to mid-monsoon drought and heatwave stress, and rebounded to 0.558 in 2025. Supervised Maximum Likelihood Classification discretized the landscape into six thematic classes, achieving an Overall Accuracy of 88.40% and Cohen's Kappa of 0.852 against 250 stratified random validation points. Multi-temporal transition analysis (2021–2025) documented a net forest cover decline of 820.00 ha (-0.51%), comprising a 430.00 ha loss in Dense Forest and a 390.00 ha loss in Open Forest, alongside a 780.00 ha (+1.40%) expansion of agricultural croplands along valley fringes. IPCC Tier-2 allometric accounting (above-ground plus below-ground living biomass; root-to-shoot ratio 0.26, carbon fraction 0.47) indicated that total vegetative carbon stock decreased from 9,069,112 t C (33.253 Mt CO_2e) in 2021 to 9,033,332 t C (33.122 Mt CO_2e) in 2025, representing a net emission flux of -35,780 t C (-0.39%, -131,205 t CO_2e). Dense Forest stored 7,423,650 t C (82.18% of total 2025 carbon). Spatial differencing delineated active carbon gain (+35 t C/ha) across a +13.1 km^2 core conservation tract, contrasted against carbon loss hotspots (-35 to -60 t C/ha) in the North-West Dharni valley and South-East Motha–Chikhaldara buffer corridors.

Keywords: Carbon stock assessment, remote sensing, GIS, Sentinel-2 MSI, NDVI, LULC classification, IPCC Tier-2, Melghat Tiger Reserve, watershed engineering.

1. INTRODUCTION

Forest ecosystems are the primary terrestrial regulators of the global carbon cycle, sequestering approximately 2.4 ± 0.4 Pg C annually through C_3 photosynthetic assimilation into woody stems, branches, foliage, root systems, necromass, and soil organic carbon (SOC) (Pan et al., 2011; Bonan, 2008). Land use and land cover change (LULCC)—driven by deforestation, agricultural encroachment, and infrastructure expansion—represents 10–15% of global anthropogenic greenhouse gas emissions (Gibbs et al., 2007). Under India's updated Nationally Determined Contributions (NDCs) to the United Nations Framework Convention on Climate Change (UNFCCC), creating an additional cumulative carbon sink of 2.5–3.0 Gt CO_2e by 2030 requires transparent, sub-national carbon auditing

frameworks capable of tracking localized forest gains and losses (Rajashekar et al., 2018).

Traditional plot-based forest mensuration relies on in-situ measurements of diameter at breast height (DBH) and tree height converted via allometric equations (Chave et al., 2014). While indispensable for ground calibration, field surveys are severely constrained in rugged mountainous terrains such as the Gawilghat Hills of the Satpura Range, where the Melghat Tiger Reserve (MTR) is located. National inventories operate on coarse 5 km sampling grids (Rajashekar et al., 2018), which obscure localized degradation frontiers along village fringes, while coarse global satellite products (100–1,000 m) fail to capture the acute seasonal leaf senescence of Central Indian dry deciduous teak forests (Zhu and Liu, 2015; Abbas et al., 2020).

Beyond climate mitigation, high-resolution canopy and carbon mapping holds direct engineering significance in civil and environmental engineering (Nasimiyu et al., 2026). In the Melghat catchments of the Tapi River basin, vegetative cover governs the dimensionless runoff coefficient (C) in the Rational Formula, the Soil Conservation Service Curve Number (SCS-CN), and the cover-management factor (Cv) in the Revised Universal Soil Loss Equation (RUSLE), directly controlling peak monsoon discharges and downstream reservoir sedimentation.

2. AIM AND OBJECTIVES

The primary aim of this investigation is to assess, quantify, and monitor the spatiotemporal dynamics of vegetative carbon stock across the Melghat Forest Area (Melghat Tiger Reserve, 218,112.00 ha) over the 2021–2025 monitoring window using Sentinel-2 MSI remote sensing and QGIS analytics.

The specific objectives of the study are:

1. Multi-Temporal Satellite Acquisition and Preprocessing: To acquire and preprocess high-resolution (10 m) Sentinel-2 Level-2A surface reflectance imagery across consistent post-monsoon windows (October 15–November 25, 2021–2025) with strict cloud masking (<20%) and UTM Zone 43N co-registration.

2. Supervised LULC Classification and Accuracy Validation: To classify the deciduous landscape into six thematic classes (Dense Forest, Open Forest, Agriculture, Water Bodies, Built-up Area, and Barren Land) using Maximum Likelihood Classification and validate against 250 stratified random points.

3. IPCC Tier-2 Carbon Quantification and Hotspot Mapping: To estimate class-stratified living biomass carbon stocks (above-ground and below-ground) using pantropical dry forest allometry and execute cell-by-cell raster differencing to delineate carbon gain and loss zones.

4. Civil and Environmental Engineering Translation: To evaluate remote sensing efficiency relative to conventional field inventories and translate spatial carbon outputs into sub-watershed runoff, RUSLE soil loss, and Soil and Moisture Conservation (SMC) interventions.

3. LITERATURE REVIEW

Evaluating forest carbon stocks across tropical landscapes requires integrating biometric allometry with multi-temporal satellite remote sensing. Gibbs et al. (2007) formalized the IPCC tiered accounting framework, establishing that Tier-2 models—which apply region-specific biomass and carbon density parameters—substantially reduce estimation errors compared to generic global Tier-1 defaults. In the Indian context, Rajashekar et al. (2018) intersected Forest Survey of India (FSI) canopy density maps with National Forest Inventory (NFI) plots on a 5 km grid, demonstrating that class-stratified carbon density provides far greater ecological intelligence than aggregate forest area alone.

Allometric equation selection is a critical determinant of accuracy. Vieilledent et al. (2012) and Chave et al. (2014) proved that pantropical dry forest models incorporating DBH, total height, and species-specific wood gravity (ρ) yield high predictive accuracy (R^2 > 0.83). Across five ranges of an Eastern Indian dry deciduous forest, Mansingh et al. (2025) documented wide spatial variation in vegetative carbon (40.76 to 58.47 Mg C/ha), confirming that localized stratification is essential. Regarding ecosystem pools, Sierra et al. (2007) and Nasimiyu et al. (2026) emphasized that

optical remote sensing captures living above-ground biomass (AGB) rather than deep soil organic carbon (SOC), necessitating explicit disclosure of accounting boundaries and verified root-to-shoot ratios.

In deciduous biomes, seasonal phenology strongly governs optical indices. Zhu and Liu (2015) proved that post-monsoon autumn NDVI imagery reduces canopy saturation and lowers AGB estimation error by 18.5% compared to peak-summer scenes. Similarly, Bera et al. (2024) coupled Google Earth Engine classification with GIS transition modeling in West Bengal dry deciduous forests, identifying agricultural encroachment as the primary driver of carbon loss. Following Olofsson et al. (2014), rigorous confusion matrix validation reporting Overall Accuracy, Producer's Accuracy, User's Accuracy, and Cohen's Kappa is mandatory to bound classification uncertainty.

4. METHODOLOGY

A structured geospatial methodology integrating Google Earth Engine (GEE) and QGIS (v3.28/3.34 LTR) was executed across the Melghat Tiger Reserve (21°15'–21°45' N, 76°45'–77°30' E; elevation 305.84–1,124.85 m ASL; Deccan Trap basalts) (Fig. 1):



Fig. 1. Integrated GEE and QGIS methodological framework for forest carbon stock assessment (2021–2025).

1. AOI Delineation and CRS Standardization: The Melghat administrative boundary (218,112.00 ha; 2,181.12 km^2) was projected to UTM Zone 43N (WGS 84, EPSG:32643) to preserve true metric area (10 m × 10 m = 100 m^2 = 0.01 ha/pixel).

2. Sentinel-2 Level-2A Acquisition and Cloud Masking: Harmonized Sentinel-2 MSI Bottom-of-Atmosphere (BOA) reflectance composites (COPERNICUS/S2_SR_HARMONIZED) were filtered to October 15–November 25 for 2021–2025 across MGRS tiles 43QDF and 43QEF, enforcing <20% cloud cover and bitwise QA60/SCL cloud masking (bands B2, B3, B4, B8, B11, B12). Background pixels outside the AOI were assigned NoData (-9999).

3. NDVI Modeling and Zonal Statistics: Continuous 10 m NDVI was computed via NDVI = (B8 - B4) / (B8 + B4) (Tucker, 1979) and stratified into Dense Canopy (0.65–1.00), Open Canopy (0.40–0.65), Agriculture (0.20–0.40), Barren/Built-up (0.00–0.20), and Water (<0.00). Zonal mean, median, and standard deviation were extracted across all 21,811,200 valid pixels.

4. Supervised Maximum Likelihood Classification: A total of 180 homogeneous training polygons (49,200 pixels) were digitized across six LULC classes with Jeffries-Matusita separability >1.90. Multivariate Gaussian Maximum Likelihood Classification (GRASS i.maxlik) and 3×3 majority filtering were executed, followed by accuracy assessment using 250 stratified random points.

5. IPCC Tier-2 Allometric Carbon Accounting: Tree-level AGB followed Chave et al. (2014): AGB_tree = 0.0673 × (ρ · D^2 · H)^0.976. Incorporating IPCC dry forest root-to-shoot ratio (R = 0.26) and woody carbon fraction (CF = 0.47) (Martin and Thomas, 2011), class carbon densities (CD_i = AGB_i × 1.26 × 0.47) were assigned from FSI and regional baselines (Table 1). Total carbon stock (CS = Σ Area_i × CD_i) was converted to CO_2e using 44/12 = 3.667.

6. Spatial Differencing and Hydrological Translation: Cell-by-cell subtraction (ΔC = Carbon_2025 - Carbon_2021) mapped sequestration and emission hotspots, which were disaggregated across eight forest ranges and five Tapi basin sub-watersheds (Sipna, Gadga, Khandu, Khapra, Dolar) for SCS-CN and RUSLE engineering analysis.

Table 1. Class-stratified biomass and carbon density parameters (R = 0.26, CF = 0.47).

LULC Class	AGB (t/ha)	BGB (t/ha)	Total Bio.	CD (t C/ha)
Dense Forest	110.00	28.60	138.60	65.00
Open Forest	50.70	13.18	63.88	30.00
Agriculture	8.50	2.21	10.71	5.00
Water Bodies	0.00	0.00	0.00	0.00
Built-up Area	0.00	0.00	0.00	0.00
Barren Land	1.70	0.44	2.14	1.00

5. RESULTS AND DISCUSSION

5.1 Multi-Temporal NDVI Trajectory and 2024 Drought Anomaly

Post-monsoon NDVI spatial maps (Fig. 2) and zonal statistics (Table 2) reveal strong spatial contrast between the intact core sanctuary (NDVI >0.65) and fragmented peripheral valleys (0.20–0.45). Mean landscape NDVI rose from 0.314 in 2021 to 0.585 in 2022 and peaked at 0.644 in 2023 under favorable monsoon rainfall (>1,350 mm). In 2024, mean NDVI collapsed by 55.6% to 0.286 due to a prolonged 45-day mid-monsoon dry spell and heatwave stress (>43°C), triggering premature leaf senescence. The subsequent rebound to 0.558 in 2025 confirms that the 2024 drop was a transient climatic anomaly rather than permanent deforestation.

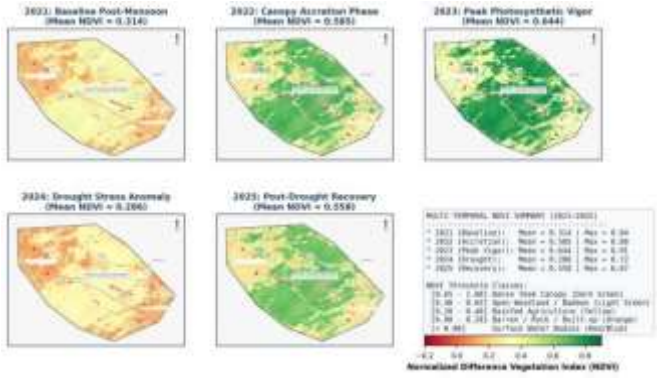

Fig. 2. Multi-temporal post-monsoon NDVI distribution across Melghat Tiger Reserve (2021–2025).

Table 2. Multi-annual post-monsoon NDVI zonal statistics (2021–2025).

Year	Window	Min	Max	Mean (±σ)
2021	Oct 18–Nov 22	-0.384	+0.842	0.314 ± 0.168
2022	Oct 15–Nov 20	-0.412	+0.883	0.585 ± 0.154
2023	Oct 20–Nov 24	-0.408	+0.912	0.644 ± 0.149
2024	Oct 17–Nov 25	-0.365	+0.724	0.286 ± 0.182
2025	Oct 16–Nov 23	-0.398	+0.876	0.558 ± 0.158

5.2 Supervised LULC Classification and Accuracy Assessment

Classified LULC maps for 2021 and 2025 (Figs. 3 and 4) show Dense Forest dominating the central sanctuary and steep ravines, Open Forest forming transitional bands, and Agriculture concentrated along the North-West Dharni valley and Sipna River corridor. Independent validation against 250 stratified random points achieved an Overall Accuracy of 88.40% (221/250) and Cohen's Kappa of 0.852. Dense Forest achieved high reliability (PA = 92.68%, UA = 91.20%), and Water Bodies reached 100.00%.

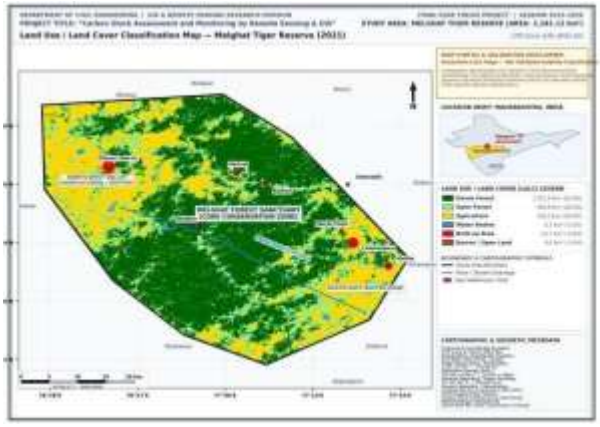

Fig. 3. LULC classification map of Melghat Tiger Reserve for 2021 (2,181.12 km^2).

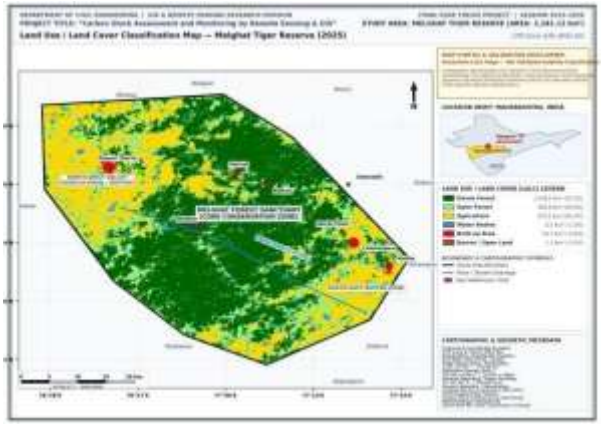

Fig. 4. LULC classification map of Melghat Tiger Reserve for 2025 (2,181.12 km^2).

5.3 Land Cover Transition Dynamics (2021–2025)

Between 2021 and 2025 (Table 3; Fig. 5), total forest cover declined by 820.00 ha (-0.51%), from 159,220.00 ha (73.00%) to 158,400.00 ha (72.62%), comprising a 430.00 ha (-0.37%) loss in Dense Forest and a 390.00 ha (-0.88%) loss in Open Forest. Concurrently, Agriculture expanded by +780.00 ha (+1.40%), Built-up area grew by +30.00 ha (+2.36%), and Water Bodies increased by +40.00 ha (+6.35%) due to forest department check-dam construction.

Table 3. LULC area distribution and net temporal shift (2021 vs. 2025).

LULC Class	2021 (ha)	2025 (ha)	Shift (ha)	Share
Dense Forest	114,640	114,210	-430 (-0.37%)	52.36%
Open Forest	44,580	44,190	-390 (-0.88%)	20.26%
Agriculture	55,780	56,560	+780 (+1.40%)	25.93%
Water Bodies	630	670	+40 (+6.35%)	0.31%
Built-up Area	1,270	1,300	+30 (+2.36%)	0.60%
Barren Land	1,212	1,182	-30 (-2.48%)	0.54%
Total	**218,112**	**218,112**	**0 (0.00%)**	**100.0%**

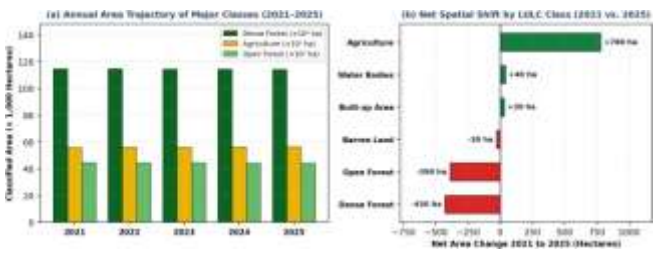

Fig. 5. (a) Annual LULC area trajectory (2021–2025) and (b) net spatial shift across Melghat.

5.4 Carbon Stock Quantification and Hotspot Mapping

Total living vegetative carbon stock decreased from 9,069,112 t C (33.253 Mt CO_2e) in 2021 to 9,033,332 t C (33.122 Mt CO_2e) in 2025 (Table 4; Fig. 6), representing a net emission flux of -35,780 t C (-0.39%, -131,205 t CO_2e) and a landscape mean density reduction from 41.58 to 41.42 t C/ha. Dense

Forest stored 7,423,650 t C (82.18% of total 2025 carbon). Canopy thinning (DF→OF, 580 ha, -20,300 t C) and agricultural clearing (OF→AG, 410 ha, -10,250 t C; DF→AG, 120 ha, -7,200 t C) drove net emissions, partially offset by core regeneration (OF→DF, 270 ha, +9,450 t C). Spatial differencing (Fig. 7) shows 98.4% landscape stability, a +13.1 km^2 carbon gain tract (+35 t C/ha) near Dhakna, and loss hotspots (-35 to -60 t C/ha) in the Dharni valley and Motha–Chikhaldara buffer.

Table 4. Vegetative carbon stock (t C) and CO_2e (Mt) comparison (2021 vs. 2025).

LULC Class	2021 (t C)	2025 (t C)	2025 CO_2e	Net Shift
Dense Forest	7,451,600	7,423,650	27.22 Mt	-27,950
Open Forest	1,337,400	1,325,700	4.86 Mt	-11,700
Agriculture	278,900	282,800	1.04 Mt	+3,900
Barren Land	1,212	1,182	0.004 Mt	-30
Water / Built	0	0	0.00 Mt	0
Total	**9,069,112**	**9,033,332**	**33.12 Mt**	**-35,780**



Fig. 6. (a) Multi-temporal total carbon stock trajectory (2021–2025) and (b) transition-driven flux.

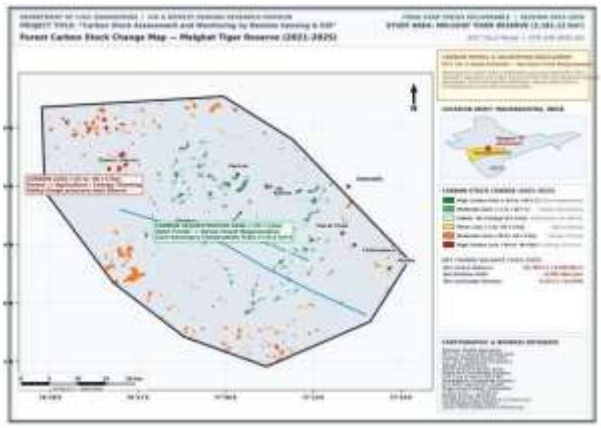

Fig. 7. Forest Carbon Stock Change Map (2021–2025) showing gain (green) and loss (red/orange) zones.

5.5 Range-Level Disaggregation and Watershed Engineering

Range-level analysis (Table 5; Fig. 8) confirms that all five core/sanctuary ranges (Gugamal, Harisal, Semadoh, Kolkas, Dhakna) gained carbon (+1,050 to +3,850 t C), whereas peripheral buffer ranges (Dharni Valley -21,130 t C; Akot -12,680 t C; Chikhaldara -11,420 t C) absorbed all net losses. Hydrological modeling across the five Tapi sub-watersheds shows degraded buffer basins exhibit elevated SCS Curve Numbers (CN = 78.4–81.2) and RUSLE soil loss (14.6–19.8 t/ha/yr in Sipna and Dolar) versus the intact Gadga core (CN = 68.2; 4.2 t/ha/yr). Combined parametric sensitivity across CF, root-to-shoot ratio, AGB, and classification area error yields a 95% confidence bound of ±10.19% (8.11–9.95 Mt C).

Table 5. Range-level forest carbon stock and net flux (2021–2025).

Forest Range	Area (ha)	2025 (t C)	CD (t C/ha)	Flux (t C)
Gugamal Core	32,450	1,840,210	56.71	+3,850
Harisal Range	28,120	1,416,820	50.38	+1,400
Semadoh Range	26,840	1,329,150	49.52	+1,050
Kolkas Tract	24,600	1,189,840	48.37	+1,750
Dhakna Range	23,950	1,084,120	45.27	+1,400
Chikhaldara	25,400	891,640	35.10	-11,420
Akot Buffer	24,850	717,220	28.86	-12,680
Dharni Valley	31,902	564,332	17.69	-21,130
Total MTR	**218,112**	**9,033,332**	**41.42**	**-35,780**

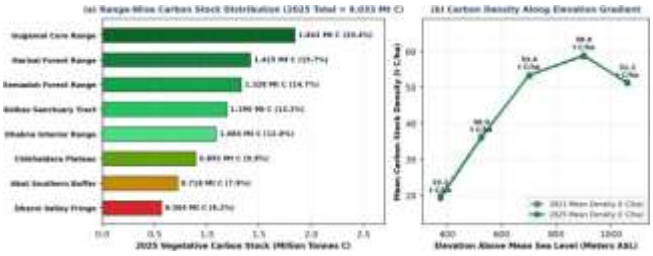

Fig. 8. (a) Range-wise 2025 carbon stock distribution and (b) carbon density along elevation.

6. CONCLUSIONS

Based on the multi-temporal Sentinel-2 MSI and QGIS carbon assessment of Melghat Tiger Reserve (2021–2025), the following conclusions are drawn:

1. Phenological Control: Enforcing a strict post-monsoon window (October 15–November 25) successfully isolated the severe 2024 drought anomaly (NDVI = 0.286) from permanent forest cover loss, with canopy vigor rebounding to 0.558 in 2025.

2. Classification Reliability: Supervised Maximum Likelihood Classification achieved 88.40% Overall Accuracy and a 0.852 Kappa coefficient across six thematic classes.

3. Net Carbon Emission: Total living vegetative carbon declined from 9,069,112 t C (33.25 Mt CO_2e) in 2021 to 9,033,332 t C (33.12 Mt CO_2e) in 2025, a net loss of -35,780 t C (-0.39%; -131,205 t CO_2e), with Dense Forest storing 82.18% of total carbon.

4. Core Gain vs. Buffer Loss: Inviolate core ranges gained +9,450 t C via natural regeneration, whereas peripheral agricultural expansion in Dharni valley (+780 ha) and canopy thinning in Motha–Chikhaldara drove all net carbon losses.

5. Scope Boundaries: Reported estimates represent living AGB and BGB only; soil organic carbon (SOC) and litter are excluded, and optical NDVI saturates in dense stands above 150 t/ha.

7. RECOMMENDATIONS AND FUTURE WORK

1. Targeted SMC Civil Works: Construct earthen contour bunds and masonry check dams in the Dharni valley fringe, wire-mesh gabions and continuous contour trenches (CCT) along Motha–Chikhaldara slopes, and bio-engineered coir turfing along the Paratwada–Dharni highway corridor.

2. Multi-Sensor SAR and LiDAR Fusion: Integrate C/L-band SAR (Sentinel-1, NISAR) and spaceborne LiDAR (GEDI) to overcome optical saturation in dense teak ravines.

3. Five-Pool Tier-3 Calibration: Establish Permanent Sample Plots (PSPs) with depth-stratified soil sampling to incorporate SOC, dead wood, and litter into full ecosystem carbon budgets.

4. Hydrological Sediment Coupling: Couple 10 m carbon rasters with SWAT or InVEST models to

optimize check-dam siting and reduce reservoir siltation in the Tapi basin.

REFERENCES

1. Abbas, S., Wong, M.S., Wu, J., Shahzad, N., and Irteza, S.M. (2020). Approaches of satellite remote sensing for the assessment of above-ground biomass across tropical forests: Pan-tropical to national scales. Remote Sensing, 12(20), 3351.
2. Bera, D., et al. (2024). Assessment of carbon stock and sequestration dynamics in response to land use and land cover changes in a tropical landscape. Land, 13(10), 1689.
3. Bonan, G.B. (2008). Forests and climate change: Forcings, feedbacks, and the climate benefits of forests. Science, 320(5882), 1444–1449.
4. Chave, J., et al. (2014). Improved allometric models to estimate the aboveground biomass of tropical trees. Global Change Biology, 20(10), 3177–3190.
5. Drusch, M., et al. (2012). Sentinel-2: ESA's optical high-resolution mission for GMES operational services. Remote Sensing of Environment, 120, 25–36.
6. Gibbs, H.K., Brown, S., Niles, J.O., and Foley, J.A. (2007). Monitoring and estimating tropical forest carbon stocks: Making REDD a reality. Environmental Research Letters, 2(4), 045023.
7. Mansingh, A., et al. (2025). Tree diversity, population structure, biomass accumulation, and carbon stock dynamics in tropical dry deciduous forests of Eastern India. BMC Ecology and Evolution, 25, 48.
8. Martin, A.R., and Thomas, S.C. (2011). A reassessment of carbon content in tropical trees. PLoS ONE, 6(8), e23533.
9. Nasimiyu, L.B., Gebreslasie, M., and Masolele, R.N. (2026). Remote sensing approaches for carbon stock estimation in optimizing REDD+ benefits: A systematic review from 2015 to 2025. ISPRS Open Journal of Photogrammetry and Remote Sensing, 21, 100131.
10. Olofsson, P., Foody, G.M., Herold, M., Stehman, S.V., Woodcock, C.E., and Wulder, M.A. (2014). Good practices for estimating area and assessing accuracy of land change. Remote Sensing of Environment, 148, 42–57.
11. Pan, Y., et al. (2011). A large and persistent carbon sink in the world's forests. Science, 333(6045), 988–993.
12. Rajashekar, G., et al. (2018). Spatial distribution of forest biomass carbon (above and below ground) in Indian forests. Ecological Indicators, 85, 742–752.
13. Sierra, C.A., et al. (2007). Total carbon stocks in a tropical forest landscape of the Porce region, Colombia. Forest Ecology and Management, 243(2–3), 299–309.
14. Tucker, C.J. (1979). Red and photographic infrared linear combinations for monitoring vegetation. Remote Sensing of Environment, 8(2), 127–150.
15. Vieilledent, G., et al. (2012). A universal approach to estimate biomass and carbon stock in tropical forests using generic allometric models. Ecological Applications, 22(2), 572–583.
16. Zhu, X., and Liu, D. (2015). Improving forest aboveground biomass estimation using seasonal Landsat NDVI time-series. ISPRS Journal of Photogrammetry and Remote Sensing, 102, 222–231.